
Lie Algebra Convolutional Networks with Automatic Symmetry Extraction

Nima Dehmamy

Northwestern University
nimadt@bu.edu

Robin Walters

Northeastern University
rsfwalters@gmail.com

Yanchen Liu

Northeastern University
liu.yanc@husky.neu.edu

Rose Qi Yu

Northeastern University
UCSD
roseyu@eng.ucsd.edu

Abstract

Existing methods for incorporating symmetries into neural network architectures require prior knowledge of the symmetry group. We propose to learn the symmetries during the training of the group equivariant architectures. Our model, the Lie algebra convolutional network (L-conv), is based on infinitesimal generators of continuous groups and does not require discretization or integration over the group. We show that L-conv can approximate any group convolutional layer by composition of layers. We demonstrate how CNNs, Graph Convolutional Networks and fully-connected networks can all be expressed as an L-conv with appropriate groups. By allowing the infinitesimal generators to be learnable, L-conv can learn potential symmetries. We also show how the symmetries are related to the statistics of the dataset in linear settings. We find an analytical relationship between the symmetry group and a subgroup of an orthogonal group preserving the covariance of the input. Our experiments show that L-conv with trainable generators performs well on problems with hidden symmetries. Due to parameter sharing, L-conv also uses far fewer parameters than fully-connected layers.

The limitations in all of the existing approaches to equivariant neural networks are: 1) they rely on knowing the symmetry group *a priori*, and 2) require encoding the whole group into the architecture. For a continuous group, it is not possible to encode all elements and we have to resort to discretization or a truncated sum over irreducible representations (irreps). Our work attempts to resolve the issues with continuous groups by using the Lie algebra (the linearization of the group near its identity) instead of the group itself. Unlike the Lie group which is infinite, the Lie algebra usually has a finite basis (notable exception being Kac-Moody Lie algebras for 2D Conformal Field Theories [2] in physics). Additionally, we show that the Lie algebra basis can be learned during training, or through a separate optimization process. Hence, our architecture, which generalizes a group convolutional layer, is potentially capable of learning symmetries in data without imposing inductive biases.

Learning symmetries in data was tackled in restricted settings of mostly commutative Lie groups as in [3] and 2D rotations and translations in [18] and [21] or permutations [1]. However, the symmetries learned by the architecture are not necessarily familiar spatial symmetries. The work that is closest in spirit and setup to ours is [28] which uses meta-learning to automatically learn symmetries. Although the weight-sharing scheme of [28] and their encoding of the symmetry generators is different, their construction does bear some resemblance to ours and we will discuss this after introducing our architecture.

Contributions Our main contributions can be summarized as follows

- We propose a group equivariant architecture using the Lie algebra, introducing the Lie algebra convolutional layer (**L-conv**).
- In L-conv the Lie algebra generators can be trained to discover symmetries, and it outperforms CNN on domains with hidden symmetries, such rotated and scrambled images.
- Group convolutional layers on connected Lie groups can be approximated by multi-layer L-conv, and fully-connected, CNN and graph convolutional networks are special cases of L-conv.

Related Work While much of the work on equivariant neural networks focuses on equivariant architectures, the ability of the architecture to discover symmetries in a given dataset is less studied. Convolutional Neural Networks (CNN) [15, 16] incorporate translation symmetry into the architecture. Recently, more general ways to construct equivariant architectures have been introduced [4, 7, 5, 14]. As a result, many other symmetries such as discrete rotations in 2D [22, 17] and 3D [5, 4] as well as permutations [27] have been incorporated into the architecture of neural networks.

Many existing works on equivariant architectures use finite groups such as permutations in [10] and [20] or discrete subgroups of continuous groups, such as 90 degree rotations in [5] or dihedral groups D_N in [23]. [19] also proved a universal approximation theorem for single hidden layer equivariant neural networks for Abelian and finite groups. General principles for constructing group convolutional layers were introduced in [7], [14], and [6], including for continuous groups. A challenge for implementation is having to integrate over the group manifold. This has been remedied either by generalizing Fast Fourier Transforms [5], or using irreps [24] either directly as spherical harmonics as in [26] or using more general Clebsch-Gordon coefficients [13]. Other approaches include discretizing the group as in [24, 25, 4], or solving constraints for equivariant irreps as in [23], or approximating the integral by sampling [8].

1 Equivariant Functions

Consider the functional mapping $\mathbf{y}_i = f(\mathbf{x}_i)$ of inputs $\mathbf{X} = (\mathbf{x}_1, \dots, \mathbf{x}_n)$ to outputs $\mathbf{Y} = (\mathbf{y}_1, \dots, \mathbf{y}_n)$. We assume each input $\mathbf{x} \in \mathbb{R}^{d \times m}$ where \mathbb{R}^d are the “space” dimensions and \mathbb{R}^m the “channels”, and $\mathbf{y} \in \mathbb{R}^c$ (or \mathbb{Z}_2^c for categorical variables). We assume a group G acts only on the space factor (\mathbb{R}^d , shared among channels) of \mathbf{x} through a d -dimensional representation $T_d : G \rightarrow \text{GL}_d(\mathbb{R})$ mapping each g to an invertible $d \times d$ matrix. The map T_d must be continuous and satisfy $T_d(u)T_d(v) = T_d(uv)$ for all $u, v \in G$ [12, IV.1]. Similarly, let G act on \mathbf{y} via a c -dimensional representation T_c . To simplify notation, we will denote the representations simply as $u_\alpha \equiv T_\alpha(u)$. A function f solving $\mathbf{y}_i = f(\mathbf{x}_i)$ is said to be equivariant under the action of a group G by representations T_c, T_d if

$$\begin{aligned} u_c \mathbf{y} &= u_c f(\mathbf{x}) = f(u_d \mathbf{x}) & \forall u \in G \\ \Leftrightarrow f(\mathbf{x}) &= u_c f(u_d^{-1} \mathbf{x}). \end{aligned} \quad (1)$$

Lie Groups and Lie Algebras The full group of invertible $d \times d$ matrices over \mathbb{R} is the general linear group, denoted as $\text{GL}_d(\mathbb{R})$. It follows that every real d -dimensional group representation $T_d(G) \subset \text{GL}_d(\mathbb{R})$. If T is a “faithful representation” (i.e. $T(u) \neq T(v)$ if $u \neq v$), then $G \subset \text{GL}_d(\mathbb{R})$.

Notation Unless stated or obvious, a in A^a is an index, not an exponent. We write matrix products as $A \cdot B \equiv \sum_a A^a B_a$. Recall that $\mathbf{x} \in \mathbb{R}^{d \times m}$. For a linear transformation $A : \mathbb{R}^{d_1} \rightarrow \mathbb{R}^{d_2}$ acting on the spatial index or the channel index, we will use one upper and one lower index as in $A_\nu^\mu h_\mu = [A \cdot h]_\nu$. We will use (a, b, c) for channels, and (μ, ν, ρ) for spatial, and (i, j, k) for Lie algebra basis indices. We will occasionally keep explicit summation \sum_i for clarity.

For any Lie group $G \subset \text{GL}_d(\mathbb{R})$, group elements infinitesimally close to the identity element can be written as $u = I + \epsilon^i L_i$. We can find a basis L_i which span the “Lie algebra” \mathfrak{g} of the group G , meaning they are closed under commutations

$$[L_i, L_j] = L_i L_j - L_j L_i = \sum_k f_{ij}^k L_k \quad (2)$$

with f_{ij}^k called the structure constants of the Lie algebra. The L_i are called the infinitesimal generators of the Lie group. They define vector fields spanning the tangent space of the manifold of G near its identity element I . For elements $u \in G_I$ in the connected component $G_I \subset G$ containing the identity, an exponential map $\exp : \mathfrak{g} \rightarrow G_I$ can be defined such that $u = \exp[t \cdot L]$. For matrix groups, if G is connected and compact, the matrix exponential defined through a Taylor expansion is such a map and it is surjective. For most other groups (except $\text{GL}_d(\mathbb{C})$ and nilpotent groups) it is not surjective. Nevertheless, for any connected group (including G_I) every element u can be written as a product $u = \prod_{\alpha} \exp[t_{\alpha} \cdot L]$ using the matrix exponential [9]. We will use this fact to modify existing results about group equivariant architectures to introduce L-conv.

2 Group Equivariant Architecture

Consider the case where the solution f to $\mathbf{y} = f(\mathbf{x})$ is implemented as a feedforward neural network. Denote the linear output of layer l by $h_l = F_l(h_{l-1}) \in \mathbb{R}^{d_l \times m_l}$, with $h_0 = x_i$. [14, 4] showed that a feedforward neural network is equivariant under the action of a group G if and only if each of its layers implement a group convolution (G-conv) given by

$$h_l = (f_l * g_l)(h_{l-1}) = \int_G d\mu(u) f_l(u_{l-1}^{-1} h_{l-1}) g_l(u) \quad (3)$$

where $d\mu(u)$ is the Haar measure on the group manifold, u_l is an appropriate d_l -dimensional representation of G , and $g_l : G \rightarrow \mathbb{R}^{m_l \times m_{l+1}}$ is a set of convolution kernels, where m_l and m_{l+1} are the number of input and output channels (filters). Here f_l are point-wise activation functions. In the formalism of [14], we may consider h_l to be a map from the homogeneous space \mathcal{X}_l to \mathbb{R}^{m_l} where \mathcal{X}_l is a space such that the space of maps $L_{\mathbb{R}}[\mathcal{X}_l]$ is parameterized by \mathbb{R}^{d_l} . To use equation 3 in practice, we need to make the integral over the group manifold tractable. Although, [8], which approximates the integral over G by sampling, approach the idea of working in the Lie algebra, they use a logarithm map to define the Lie algebra. We take a different approach and formulate the architecture in terms of the Lie algebra basis. We also allow the architecture to learn basis L_i for the symmetries.

For continuous symmetry groups, we show that using the Lie algebra can approximate G-conv without having to integrate over the full group manifold, thus alleviating the need to discretize or sample the group. The key point is the discreteness and finiteness of the Lie algebra basis for many Lie groups.

Proposition 1. *Let G be a Lie group and $T_d : G \rightarrow \mathbb{R}^{d_l}$ a d_l -dimensional representation of G . If a convolution kernel $g_l : G \rightarrow \mathbb{R}^{m_{l-1} \times m_l}$ has support only on an infinitesimal η neighborhood of identity, a G-conv layer of equation 3 can be written in terms of the Lie algebra.*

Proof: Linearization over η yields $u_l \approx I + \epsilon \cdot L$ in equation 3, with $L_i \in \mathbb{R}^{d_l \times d_l}$. The inverse is then $u_l^{-1} \approx I - \epsilon \cdot L + O(\epsilon^2)$.

Since g_l has support only in an η neighborhood of identity, fixing a basis L_i , we can reparametrize $g_l(I + \epsilon \cdot L) = \tilde{g}_l(\epsilon)$ as a function over the Lie algebra $\tilde{g}_l : \mathfrak{g} \rightarrow \mathbb{R}^{m_{l-1} \times m_l}$. Dropping the layer index l for brevity, we have

$$(f * g)(h) \approx \int_G \tilde{g}(\epsilon) f((I - \epsilon \cdot L)h) d^{m_L} \epsilon \approx (W^0 I - W \cdot L) h \cdot \nabla_h f(h) \quad (4)$$

$$W^0 \equiv \int_G \tilde{g}(\epsilon) d^{m_L} \epsilon, \quad W^i \equiv \int_G \epsilon^i \tilde{g}(\epsilon) d^{m_L} \epsilon. \quad (5)$$

where the number of W^i is n_L , the number of L_i . When $f(h)$ is a homogeneous function like ReLU or linear activation, $h \cdot \nabla_h f(h) = a f(h)$. In general, since we are designing the layers, we can choose $h \cdot \nabla_h f(h) = \sigma(h)$ to be a desired activation function. \square

Note that in G-conv, the convolutional kernels $g(u)$ are the trainable weights. The difficulty with learning them is that one has to parametrize and integrate the convolution over the group G . The major advantage of working in the Lie algebra instead of G is that in equation 4 the integrals of $g(\epsilon)$ separate from $f(h)$, leaving us with a set of integrated weights W . This means that instead of the architecture needing to implement the integral $\int_G g(u) f(uh) d\mu$, we only need to learn a finite number of convolutional weights W , like the filter weights in CNN. Additionally, we can learn L_i . Indeed, having learnable L_i to learn hidden symmetries is one of main features we are proposing, as we show in our experiments.

L-conv Layer The construction in equation 4 is at the core of our results. $h \in \mathbb{R}^{d_{l-1} \times m_{l-1}}$ has components h_μ^a , where $\mu \in \{1, \dots, d_{l-1}\}$ is the spatial index and $a \in \{1, \dots, m_{l-1}\}$ the channel index. We define the Lie algebra convolutional layer (L-conv) as

$$\begin{aligned} \text{L-conv : } F_L(h) &= \sigma \left(\sum_{i=0}^{n_L} L_i \cdot h \cdot W^i + b \right) \\ F_L(h)_\mu^a &= \sigma \left(\sum_{i,\nu,c} [L_i]_\mu^\nu h_\nu^c [W^i]_c^a + b^a \right) \end{aligned} \quad (6)$$

where σ is the activation function, $L_0 = I$ and $W^i \in \mathbb{R}^{m_l \times m_{l-1}}$ are the convolutional weights, and the second line shows the components (all symbols are indices, not exponents). Note that, similar to discussion in [24], an arbitrary nonlinear activation σ may not keep the architecture equivariant under G , but linear activation remains equivariant. Also, note that in equation 3, f_l is the activation σ_{l-1} of the previous layer. In defining L-conv we are including the activation σ after the convolution, which is why σ appears outside in equation 6 instead of as $\sigma(h)$.

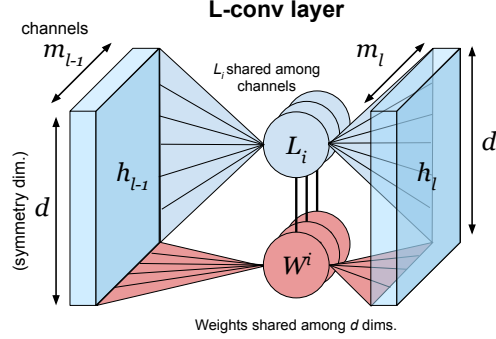


Figure 1: L-conv layer architecture. L_i only act on the d spatial dimensions, and W^i only act on the m_l feature. For each i , this action is analogous to a Graph Convolutional Network with d nodes and m_l features per node.

Since in connected Lie groups larger group elements can be constructed as $u = \prod_{\alpha} \exp[t_{\alpha} \cdot L]$ [9] from elements near identity, it follows that any G-conv layer can be constructed from multiple L-conv layers on these groups.

Proposition 2. Any G-conv layer on a connected Lie group can be approximated by a multi-layer L-conv to arbitrary accuracy.

So far we have shown that L-conv layers could replace G-conv for connected groups. The advantage of using L-conv layers is that for many potential symmetry groups, such as orthogonal and unitary groups, the number of generators L_i is finite and often a small number of them may be sufficient. For instance, consider $SO(2)$ rotations on $p \times p$ images. The flattened image has $d = p^2$ dimensions and the number of $GL_d(\mathbb{R})$ generators is p^4 . However the induced representation of $SO(2)$ on \mathbb{R}^d has a single generator. In fact, in many domains we expect symmetries hidden in the data to be much lower in dimensionality than the data itself. Additionally, in the other extreme, where there is no restriction on the symmetry, meaning $G = GL_d(\mathbb{R})$, we observe that L-conv becomes a fully-connected layer, as shown next.

Proposition 3. A fully-connected neural network layer can be written as an L-conv layer using $GL_d(\mathbb{R})$ generators, followed by a sum pooling and nonlinear activation.

Thus, interestingly, more restricted groups, rather than large, meaning groups with fewer L_i , lead to more parameter sharing. Indeed, as we show below, the most restricted L-conv are graph convolutional networks. It is also easy to see that familiar CNN can be encoded as L-conv. Note that, generally shift operators used in CNN are thought of as group elements for a discrete permutation group. However, the same shift operators L_i can be used to create continuous fractional shifts as $(I + \alpha L_i)/(\alpha + 1)$. Since shifts commute with each other, they form a basis for the Lie algebra of an Abelian subgroup of $GL_d(\mathbb{R})$.

Proposition 4. CNN is a special case of L-conv where the generators are shift operators.

In CNN, covering larger patches is equivalent to $g(u)$ covering a larger part of the group. But large convolutional kernels are not generally used. Instead, we achieve larger receptive fields by adding more CNN layers, similar to Proposition 2.

Connection with Graph Convolutional Networks Finally, we note that the L-conv layer equation 6 has the structure of a Graph Convolutional Networks (GCN) [11] with multiple propagation

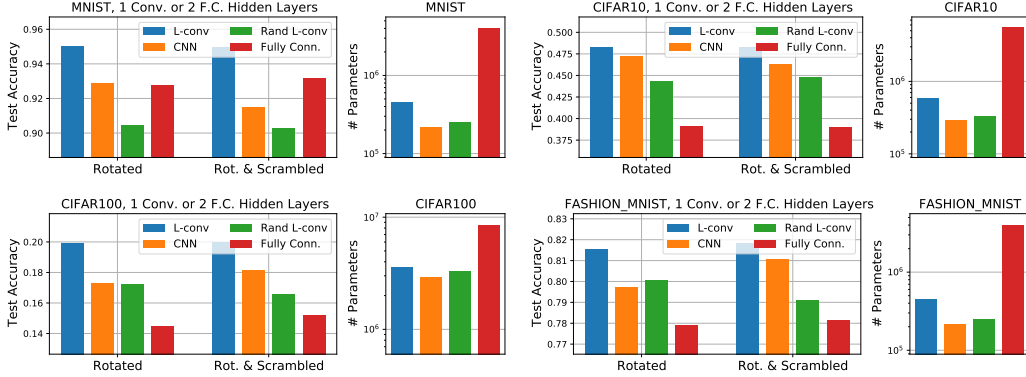


Figure 2: Test results on four datasets with two variant: “Rotated” and “Rotated and scrambled”. In all cases L-conv performed best. In MNIST, FC and CNN layers come close, but using 5x more parameters.

rules L_i derived from graph adjacency matrices and μ, ν indexing graph vertices. Thus, an L-conv with a single L is a GCN. In fact, there is a deeper connection here, as we show now.

Proposition 5. *A GCN with propagation rule $A \in \mathbb{R}^{d \times d}$ is equivalent to an L-conv, with the group being 1D flows generated by $A - I$.*

Hence, the most restricted L-conv based on 1D flow groups with a single generator are GCN. These flow groups include Hamiltonian flows and other linear dynamical systems. CNN can also be interpreted as a GCN with multiple propagation rules, where each shift operator is a subgraph of the grid network.

3 Learning Potential Symmetries

When dealing with unknown continuous symmetry groups, it can be virtually impossible to design a G-conv, as it relies on the structure of the group. The Lie algebra, however, has a much simpler, linear structure and universal for all Lie groups. Because of this, L-conv affords us with a powerful tool to probe systems with unknown symmetries. L-conv is a generic weight-sharing ansatz and the number of L_i can be expected to be small in many systems. This means that even if we do not know L_i , it may be possible to *learn* the L_i from the data. In fact, as we show in our experiments, learnable low-rank L_i yield impressive performance on data with hidden symmetries (Fig. 2), without needing any input about the symmetry. (See Appendix B for comparison with MSR [28])

Learning the L_i We learn the L_i using SGD, simultaneously with W^i and all other weights. Our current implementation is similar to a GCN $F(h) = \sigma(L_i \cdot h \cdot W^i + b)$ where both the weights W^i and the propagation rule L_i are learnable. When the spatial dimensions d of the input $x \in \mathbb{R}^{d \times c}$ is large, e.g. a flattened image, the L_i with d^2 parameters can become expensive to learn. However, generators of groups are generally very sparse matrices. Therefore, we represent L_i using low-rank decomposition $L_i = U_i V_i$. An encoder V of shape $n_L \times d_h \times d$ encodes n_L matrices V_i , and a decoder U of shape $n_L \times d \times d_h$. Here d is the input dimensions and d_h the latent dimension with $d_h \ll d$ for sparsity. In order for the L_i to form a basis for a Lie algebra, they should be closed under the commutation relations equation 2, as well as orthogonal under the Killing Form [9, Chapter 6]. These conditions can be added to the model as regularizers, but regularization also introduces an additional time complexity of $O(n_L^2 d_h^2 d)$, which can be quite expensive compared to the $O(n_L d_h d)$ of learning L_i via SGD. Therefore, in the experiments reported here we did not use any regularizers for L_i .

4 Experiments

See Appendix C for more details on the model, baselines and experiment setup.

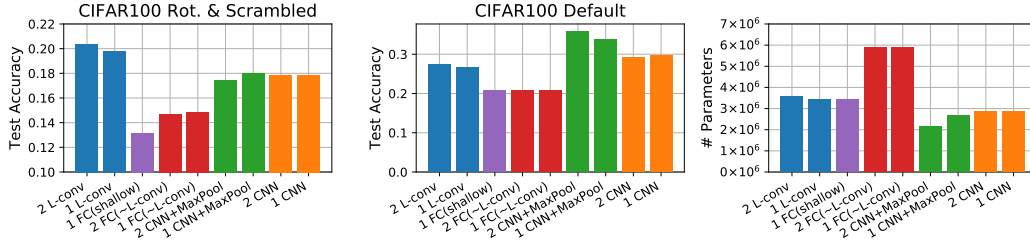


Figure 3: Comparison of one and two layer performance of L-conv (blue), CNN without pooling (orange), CNN with Maxpooling after each layer (green), fully connected (FC) with structure similar to L-conv (red) and shallow FC, which has a single hidden layer with width such that the total number of parameters matches L-conv (purple). The labels indicate number of layers and layer architecture (e.g. “2 L-conv” means two layers of L-conv followed by one classification layer). Left and middle plots show test accuracies on CIFAR100 with rotated and scrambled images, and on the original CIFAR100 dataset, respectively. The plot on the right show the number of parameters of each model, which is the same for the two datasets.

Test Datasets We used four datasets: MNIST, CIFAR10, CIFAR100, and FashionMNIST. To test efficiency of L-conv in dealing with hidden or unfamiliar symmetries, we conducted our tests on two modified versions of each dataset: 1) **Rotated**: each image rotated by a random angle (no augmentation); 2) **Rotated and Scrambled**: random rotations are followed by a fixed random permutation (same for all images) of pixels. **Baselines** We compare L-conv against three baselines: CNN, random L_i , and FC.

Learning L_i during Training When the spatial dimensions d of the input $x \in \mathbb{R}^{d \times c}$ is large, e.g. a flattened image, the L_i with d^2 parameters can become expensive to learn. However, generators of groups are generally very sparse matrices. Therefore, we encode the L_i with an autoencoder structure with one or multiple hidden dimensions. The hidden bottleneck allows for low-rank encoding of the L_i . In practice, we find that a single hidden layer with linear activation and very low dimensions (hidden width 6 on rotated and scrambled MNIST) worked best in our tests.

Results The results of our test are shown in Fig. 2. As we see, on all four datasets both in the rotated and the rotated and scrambled case L-conv performed considerably better than CNN and the rest of the baselines. We are also showing the total number of trainable parameters in L-conv and other model next to the accuracy plot using the same colors. L-conv naturally requires parameters to encode L_i , but low-rank encoding with rank $k \ll d$ only requires $O(kd)$ parameters, which can be negligible compared to FC layers. We also ran tests on the unmodified images, (shown in Supp. Fig 4), where CNN performed best, but L-conv closely trailed it.

Additional experiments testing the effect of number of layers, number of parameters and pooling are shown in Fig. 3. On CIFAR100, we find that both FC configurations, FC(∼L-conv) and FC(shallow) consistently perform worse than L-conv, evidence that L-conv’s performance is *not* due to its extra parameters. L-conv outperforms all other tested models on rotated and scrambled CIFAR100. Without pooling, we observe that both L-conv and CNN do not benefit from adding a second layer. This can be explained by Proposition 2, which states that multi-layer L-conv is still encoding the same symmetry group G , only covering a larger portion of G . Our hypothesis is that lack of pooling is the reason behind this, as we discuss next.

Pooling on L-conv On Default CIFAR100, CNN with Maxpooling significantly outperforms regular CNN and L-conv, indicating the importance of proper pooling. Interestingly, on rotated and scrambled CIFAR100, we find that max-pooling does not yield any improvement. We believe the role of pooling is much more fundamental than simple dimensionality reduction. On images, pooling with strides blurs our low-level features, allowing the next layer to encode symmetries at a larger scale. [4] showed a relation between pooling and coset of subgroups and that strides are subsampling the group to a subgroup $H \subset G$, resulting in outputs which are equivariant only under H and not the full G . These subgroups appearing at different scales in the data may be quite different. However, a naive implementation of pooling on L-conv may involve three L_i and be quite expensive. Devising an efficient and mathematically sound pooling algorithm for L-conv is a future step we are working on.

5 Discussions

We introduced the L-conv layer, a group equivariant layer based on Lie algebras of continuous groups. We showed that many familiar architectures such as CNN, GCN and FC layers can be understood as L-conv. L-conv is easy to setup and can learn symmetries during training. On domains with hidden symmetries, we find that an L-conv layer outperforms other comparable baseline layer architectures. L-conv can in principle be inserted anywhere in an architecture. L-conv can also be composed in multiple layers, though Proposition 2 suggests it would be approximating the same symmetry group, and we did not observe significant improvements in performance in our multilayer tests. For CNN on images, coarse-graining (maxpooling with strides) allows the system to find features at a different scale, whose symmetry may be a subset of the lower scale [4] or perhaps new symmetries. Thus, one future work direction is defining proper pooling. Lastly, to ensure L_i behave like a Lie algebra basis, we need to include regularizers enforcing orthogonality among the L_i , which is another future direction.

References

- [1] Fabio Anselmi, Georgios Evangelopoulos, Lorenzo Rosasco, and Tomaso Poggio. Symmetry-adapted representation learning. *Pattern Recognition*, 86:201–208, 2019.
- [2] Alexander A Belavin, Alexander M Polyakov, and Alexander B Zamolodchikov. Infinite conformal symmetry in two-dimensional quantum field theory. *Nuclear Physics B*, 241(2):333–380, 1984.
- [3] Taco Cohen and Max Welling. Learning the irreducible representations of commutative lie groups. In *International Conference on Machine Learning*, pages 1755–1763, 2014.
- [4] Taco Cohen and Max Welling. Group equivariant convolutional networks. In *International conference on machine learning*, pages 2990–2999, 2016.
- [5] Taco S Cohen, Mario Geiger, Jonas Köhler, and Max Welling. Spherical cnns. *arXiv preprint arXiv:1801.10130*, 2018.
- [6] Taco S Cohen, Mario Geiger, and Maurice Weiler. A general theory of equivariant cnns on homogeneous spaces. In *Advances in Neural Information Processing Systems*, pages 9142–9153, 2019.
- [7] Taco S Cohen and Max Welling. Steerable cnns. *arXiv preprint arXiv:1612.08498*, 2016.
- [8] Marc Finzi, Samuel Stanton, Pavel Izmailov, and Andrew Gordon Wilson. Generalizing convolutional neural networks for equivariance to lie groups on arbitrary continuous data. *arXiv preprint arXiv:2002.12880*, 2020.
- [9] Brian Hall. *Lie groups, Lie algebras, and representations: an elementary introduction*, volume 222. Springer, 2015.
- [10] Jason Hartford, Devon R Graham, Kevin Leyton-Brown, and Siamak Ravanbakhsh. Deep models of interactions across sets. *arXiv preprint arXiv:1803.02879*, 2018.
- [11] Thomas N Kipf and Max Welling. Semi-supervised classification with graph convolutional networks. *arXiv preprint arXiv:1609.02907*, 2016.
- [12] Anthony W Knapp. *Lie groups beyond an introduction*, volume 140. Springer Science & Business Media, 2013.
- [13] Risi Kondor, Zhen Lin, and Shubhendu Trivedi. Clebsch–gordan nets: a fully fourier space spherical convolutional neural network. In *Advances in Neural Information Processing Systems*, pages 10117–10126, 2018.
- [14] Risi Kondor and Shubhendu Trivedi. On the generalization of equivariance and convolution in neural networks to the action of compact groups. *arXiv preprint arXiv:1802.03690*, 2018.
- [15] Yann LeCun, Bernhard Boser, John S Denker, Donnie Henderson, Richard E Howard, Wayne Hubbard, and Lawrence D Jackel. Backpropagation applied to handwritten zip code recognition. *Neural computation*, 1(4):541–551, 1989.
- [16] Yann LeCun, Léon Bottou, Yoshua Bengio, and Patrick Haffner. Gradient-based learning applied to document recognition. *Proceedings of the IEEE*, 86(11):2278–2324, 1998.

- [17] Diego Marcos, Michele Volpi, Nikos Komodakis, and Devis Tuia. Rotation equivariant vector field networks. In *Proceedings of the IEEE International Conference on Computer Vision*, pages 5048–5057, 2017.
- [18] Rajesh PN Rao and Daniel L Ruderman. Learning lie groups for invariant visual perception. In *Advances in neural information processing systems*, pages 810–816, 1999.
- [19] Siamak Ravanbakhsh. Universal equivariant multilayer perceptrons. *arXiv preprint arXiv:2002.02912*, 2020.
- [20] Siamak Ravanbakhsh, Jeff Schneider, and Barnabas Poczos. Equivariance through parameter-sharing. In *Proceedings of the 34th International Conference on Machine Learning-Volume 70*, pages 2892–2901. JMLR. org, 2017.
- [21] Jascha Sohl-Dickstein, Ching Ming Wang, and Bruno A Olshausen. An unsupervised algorithm for learning lie group transformations. *arXiv preprint arXiv:1001.1027*, 2010.
- [22] Bastiaan S Veeling, Jasper Linmans, Jim Winkens, Taco Cohen, and Max Welling. Rotation equivariant cnns for digital pathology. In *International Conference on Medical image computing and computer-assisted intervention*, pages 210–218. Springer, 2018.
- [23] Maurice Weiler and Gabriele Cesa. General e (2)-equivariant steerable cnns. In *Advances in Neural Information Processing Systems*, pages 14334–14345, 2019.
- [24] Maurice Weiler, Mario Geiger, Max Welling, Wouter Boomsma, and Taco S Cohen. 3d steerable cnns: Learning rotationally equivariant features in volumetric data. In *Advances in Neural Information Processing Systems*, pages 10381–10392, 2018.
- [25] Maurice Weiler, Fred A Hamprecht, and Martin Storath. Learning steerable filters for rotation equivariant cnns. In *Proceedings of the IEEE Conference on Computer Vision and Pattern Recognition*, pages 849–858, 2018.
- [26] Daniel E Worrall, Stephan J Garbin, Daniyar Turmukhambetov, and Gabriel J Brostow. Harmonic networks: Deep translation and rotation equivariance. In *Proceedings of the IEEE Conference on Computer Vision and Pattern Recognition*, pages 5028–5037, 2017.
- [27] Manzil Zaheer, Satwik Kottur, Siamak Ravanbakhsh, Barnabas Poczos, Russ R Salakhutdinov, and Alexander J Smola. Deep sets. In *Advances in neural information processing systems*, pages 3391–3401, 2017.
- [28] Allan Zhou, Tom Knowles, and Chelsea Finn. Meta-learning symmetries by reparameterization. *arXiv preprint arXiv:2007.02933*, 2020.

A Proofs

Proposition 1

Proof: (Extended) Linearization over η yields $u_l \approx I + \epsilon \cdot L$ in equation 3, with $L_i \in R^{d_l \times d_l}$. The inverse is then $u_l^{-1} \approx I - \epsilon \cdot L + O(\epsilon^2)$. The convolution kernels $g_l(u)$ are functions defined on the group manifold. Since every group element can be constructed from the Lie algebra through the exponential map $u = \exp[t \cdot L]$, any function on the group can be parametrized using the same t , as $g(u) = \tilde{g}(t)$. For example in three dimensional rotations $SO(3)$, the t are angles θ, ϕ and $\tilde{g}(t)$ can be expanded using spherical harmonics $Y_l^m(\theta, \phi)$. In non-abelian groups, for elements far away from identity there will be path dependence in the parametrization and $\exp[t \cdot L]$ is defined through Dyson series, for elements near identity, a simple linear expansion is unambiguous.

Since g_l has support only in an η neighborhood of identity, fixing a basis L_i , we can reparametrize $g_l(I + \epsilon \cdot L) = \tilde{g}_l(\epsilon)$ as a function over the Lie algebra $\tilde{g}_l : \mathfrak{g} \rightarrow \mathbb{R}^{m_l \times m_l+1}$. Dropping the layer index l for brevity, we have

$$\begin{aligned} (f * g)(h) &\approx \int_G \tilde{g}(\epsilon) f((I - \epsilon \cdot L)h) d^{m_L} \epsilon \\ &\approx (W^0 I - W \cdot L) h \cdot \nabla_h f(h) \end{aligned} \quad (7)$$

$$W^0 \equiv \int_G \tilde{g}(\epsilon) d^{m_L} \epsilon, \quad W^i \equiv \int_G \epsilon^i \tilde{g}(\epsilon) d^{m_L} \epsilon. \quad (8)$$

where the number of W^i is n_L , the number of L_i . When $f(h)$ is a homogeneous function like ReLU or linear activation, $h \cdot \nabla_h f(h) = af(h)$. In general, since we are designing the layers, we can choose $h \cdot \nabla_h f(h) = \sigma(h)$ to be a desired activation function. \square

Proposition 2

Proof: To show this we need to take two steps. First, we discretize the support of $g(u)$ in equation 3 to infinitesimally small sets $G = \bigcup_k G_k$, each having support around an element $u_k \in G_k$. This allows us to write $(f * g)(h) \approx \sum_k \Delta\mu_k g(u_k) f(u_k^{-1}h)$, where $\Delta\mu_k = \int_{G_k} d\mu$. Next, we write each u_k as a product. On connected groups for any $u_k \in G$, we can write $u_k = \prod_{\alpha=1}^l v_\alpha$ where $v_\alpha = \exp[t_\alpha \cdot L] \approx (I + t_\alpha \cdot L)$ are elements close to identity. Then, $f(uh)$ can be written as a composition l G-conv layers, each with weights $g_\alpha(u) = \delta(u - v_\alpha)$ (defined using a faithful representation of G)

$$f(u_k^{-1}h) = f\left(\prod_{\alpha} v_\alpha h\right) = f(F_l \circ \dots \circ F_1(h)), \quad F_\alpha(h) = \int_G d\mu(u) f_\alpha(u_\alpha h) g_\alpha(u) \quad (9)$$

Since u_α are near identity, each F_α can be converted to an L-conv layer with linear activation and weights $W = t_\alpha$ and $W^0 = 1$. Thus, the G-conv layer can be approximated as sum and composition of L-conv layers. Each G_k can be considered one output channel for the multi-layer L-conv and $g(u_k)$ are weights of a final aggregation layer. \square

Proposition 3

Proof: The generators of $GL_d(\mathbb{R})$ are one-hot $\mathbf{E} \in \mathbb{R}^{d \times d}$ matrices $L_i = \mathbf{E}_{(\alpha, \beta)}$ which are non-zero only at index $i = (\alpha, \beta)$ ¹ with elements written using Kronecker deltas

$$GL_d(\mathbb{R}) \text{ generators : } L_{i, \mu}^\nu = [\mathbf{E}_{(\alpha, \beta)}]_\mu^\nu = \delta_{\mu\alpha} \delta_\beta^\nu \quad (10)$$

Now, consider the weight matrix $w \in \mathbb{R}^{m \times d}$ and bias $b \in \mathbb{R}^m$ of a fully connected layer acting on $h \in \mathbb{R}^d$ as $F(h) = \sigma(w \cdot h + b)$. The matrix element can be written as

$$w_b^\nu = \sum_{\mu} \sum_{\alpha, \beta} w_b^\alpha \mathbf{1}_\beta [\mathbf{E}_{(\alpha, \beta)}]_\mu^\nu = \sum_{\mu} \sum_{\alpha, \beta} W_{(\alpha, \beta)}^{b, 1} [\mathbf{E}_{(\alpha, \beta)}]_\mu^\nu = \sum_{\mu} W^{b, 1} \cdot [L]_\mu^\nu \quad (11)$$

meaning an L-conv layer with weights $W_{(\alpha, \beta)}^{b, 1} = w_b^\alpha \mathbf{1}_\beta$ (1 input channel, and $\mathbf{1}$ being a vector of ones) followed by pooling over μ is the same as a fully connected layer with weights w . \square

¹We may also label them by single index like $i = \alpha + \beta d$, but two indices is more convenient.

Proposition 4

Proof: In 1D CNN, for a kernel size k we have k shift operators L_i given by $L_{i\mu}^\nu = \delta_{\mu,\nu-i}$. Plugging this into equation 6 and doing the sum over ν , we recover the convolution formula

$$F(h)_\mu^a = \sigma \left(\sum_{i,c} h_{\mu-i}^c W_c^{i,a} + b^a \right) \quad (12)$$

In higher dimensional CNN, i covers the relevant flattened indices for the required shifts. For instance, a $p \times q$ image, when flattened becomes a vector of length pq . To cover a $(2, 2)$ convolutional kernel, we need shifts to be by $0, 1, q, q + 1$ pixels. Thus, we need four L_i given by

$$L_{i\mu}^\nu = \delta_{\mu,\nu-s_i}, \quad s_i = [0, 1, q, q + 1]_i \quad (13)$$

This means that the number of generators L_i is the size of the convolutional kernel in CNN. Generalization to higher dimensions is straightforward. \square

Proposition 5

Proof: We can define a linear flow similar to a diffusion equation

$$h(t + \delta t) = Ah_\nu(t) \quad \Rightarrow \quad \frac{dh(t)}{dt} = \lambda(A - I)h(t) \quad (14)$$

where $\lambda = \delta t / dt$ sets the time scale. Thus $L = \lambda(A - I)$ is the generator a 1D group of flows with elements $u = \exp[tL]$, a subgroup of the group of diffeomorphisms on \mathbb{R}^d , with a single generator L . Thus, a GCN with propagation rule A is an L-conv using $L_0 = I$ and $L_1 = L$ with the same convolutional weights for L_0, L_1 . \square

B Comparison with Meta-learning Symmetries by Reparameterization (MSR)

Recently [28] also introduced an architecture which can learn equivariences from data. We would like to highlight the differences between their approach and ours, specifically Proposition 1 in [28]. Assuming a discrete group $G = \{g_1, \dots, g_n\}$, they decompose the weights $W \in \mathbb{R}^{s \times s}$ of a fully-connected layer, acting on $x \in \mathbb{R}^s$ as $\text{vec}(W) = U^G v$ where $U^G \in \mathbb{R}^{s \times s}$ are the ‘‘symmetry matrices’’ and $v \in \mathbb{R}^s$ are the ‘‘filter weights’’. Then they use meta-learning to learn U^G and during the main training keep U^G fixed and only learn v . We may compare MSR to our approach by setting $d = s$. First, note that although the dimensionality of $U \in \mathbb{R}^{nd \times d}$ seems similar to our $L \in \mathbb{R}^{n \times d \times d}$, the L_i are n matrices of shape $d \times d$, whereas U has shape $(nd) \times d$ with many more parameters than L . Also, the weights of L-conv $W \in \mathbb{R}^{n \times m_l \times m_l - 1}$, with m_l being the number of channels, are generally much fewer than MSR filters $v \in \mathbb{R}^d$. Finally, the way in which Uv acts on data is different from L-conv, as the dimensions reveal. The prohibitively high dimensionality of U requires MSR to adopt a sparse-coding scheme, mainly Kronecker decomposition. Though not necessary, we too choose to use a sparse format for L_i , finding that very low-rank L_i often perform best. A Kronecker decomposition may bias the structure of U^G as it introduces a block structure into it.

C L-conv Experiments

Test Datasets We used four datasets: MNIST, CIFAR10, CIFAR100, and FashionMNIST. To test efficiency of L-conv in dealing with hidden or unfamiliar symmetries, we conducted our tests on two modified versions of each dataset: 1) **Rotated**: each image rotated by a random angle (no augmentation); 2) **Rotated and Scrambled**: random rotations are followed by a fixed random permutation (same for all images) of pixels. We used a 80-20 training test split on 60,000 MNIST and FashionMNIST, and on 50,000 CIFAR10 and CIFAR100 images. Scrambling destroys the correlations existing between values of neighboring pixels, removing the locality of features in images. As a result, CNN need to encode more patterns, as each image patch has a different correlation pattern.

Baselines We compare L-conv against three baselines: CNN, random L_i , and FC. Using CNN on scrambled images amounts to using poor inductive bias in designing the architecture. Similarly, random, untrained L_i is like using bad inductive biases. One reason we test on random L_i is to verify

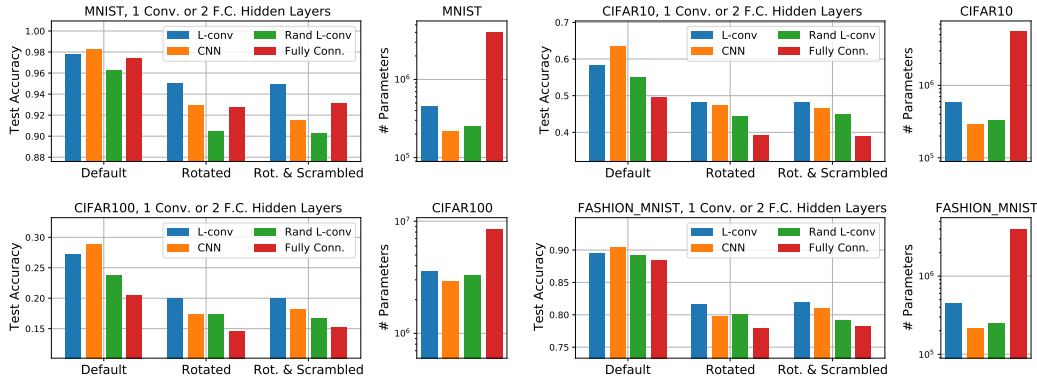


Figure 4: Test results on four datasets with three variant: “Default” (unmodified dataset), “Rotated” and “Rotated and scrambled”. On the Default dataset, CNN performs best, but L-conv is always the second best. For Rotated and Rot. & Scrambled, in all cases L-conv performed best. In MNIST, FC and CNN layers come close, but using 5x more parameters.

that any improvement in performance is not somehow due to the structure of the architecture, rather than L-conv really learning symmetry patterns. Finally, to verify that the higher parameter count in L-conv is not responsible for the high performance, we construct multilayer fully-connected networks with the same input ($d \times m_0$), hidden ($k \times n_L$ for low-rank L_i) and output dimensions ($d \times m_1$) as L-conv, but lacking the weight-sharing, which leads to much larger number parameters.

Learning L_i during Training When the spatial dimensions d of the input $x \in \mathbb{R}^{d \times c}$ is large, e.g. a flattened image, the L_i with d^2 parameters can become expensive to learn. However, generators of groups are generally very sparse matrices. Therefore, we encode the L_i with an autoencoder structure with one or multiple hidden dimensions. The hidden bottleneck allows for low-rank encoding of the L_i . In practice, we find that a single hidden layer with linear activation and very low dimensions (hidden width 6 on rotated and scrambled MNIST) worked best in our tests.

Test Model Architectures We conduct controlled tests, with a single hidden layer being either L-conv or the baseline layers, followed by a classification layer. For CNN, L-conv and random L_i L-conv, we used $m_1 = 32$ for number of output filters. For CNN we used 3×3 kernels and equivalently used $n_L = 9$ for the number of L_i in L-conv and random L-conv. For low-rank encoding of L_i we used $k = 16$, although lower values like $k = 6$ had similar performance.

Results The results of our test are shown in Fig. 2. As we see, on all four datasets both in the rotated and the rotated and scrambled case L-conv performed considerably better than CNN and the rest of the baselines. We are also showing the total number of trainable parameters in L-conv and other model next to the accuracy plot using the same colors. L-conv naturally requires parameters to encode L_i , but low-rank encoding with rank $k \ll d$ only requires $O(kd)$ parameters, which can be negligible compared to FC layers. We also ran tests on the unmodified images, (shown in Supp. Fig 4), where CNN performed best, but L-conv closely trailed it.

Hardware and Implementation We implemented L-conv in Keras and Tensorflow 2.2 and ran our tests on a system with a 6 core Intel Core i7 CPU, 32GB RAM, and NVIDIA Quadro P6000 (24GB RAM) GPU. The L-conv layer did not require significantly more resources than CNN and ran only slightly slower.

In Figure 5 we compare the performance of a single layer of L-conv on a classification task on scrambled rotated MNIST, where pixels have been permuted randomly and images have been rotated between -90 to $+90$ degrees. The models consisted of a final classification layer preceded by either one L-conv (blue), or one CNN (orange), or multiple fully-connected (FC, green) layers with similar number of neurons as the L-conv, but without weight sharing. We see that most L-conv configurations had the highest performance without a too many trainable parameters. Note that, parameters in FC layers are much higher than comparable L-conv, but yield worse results. The dots are labeled to show the configurations, with $L[32]h[6](k[6])$ meaning $k = 6$ as number of L_i , 32 output filters, and $h = 6$ hidden dimensions for low-rank encoding of L_i . The y-axis shows the test accuracy and the

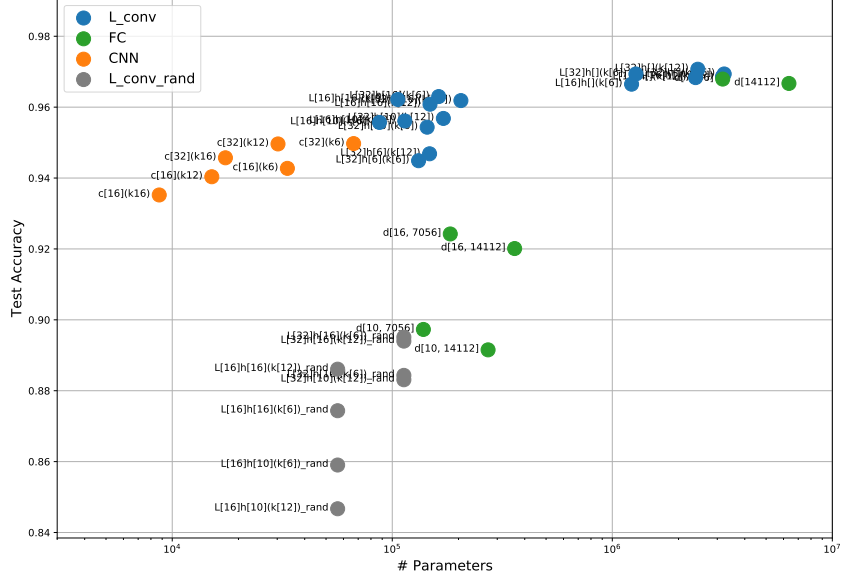


Figure 5: Training low-rank L-conv layer during training.

x-axis the number of trainable parameters. The grey lines show the performance of L-conv with fixed random L_i , but trainable shared wights, showing that indeed the learned L_i improve the performance quite significantly.

C.1 Symmetries of Linear Regression

Next, we will show that in certain cases, such as linear regression, a subset of continuous symmetries can be derived analytically. While the results may not apply to more non-linear cases, they give us a good idea of the nature of the symmetries we should expect L-conv to learn.

In the case of linear regression we can derive part of the symmetries explicitly, as shown next. For brevity, we absorb biases into the regression weights \mathbf{A} as the last row and append a row of 1 to the input.

Theorem 1. Consider a linear regression problem on inputs $\mathbf{X} \in \mathbb{R}^{d \times n}$ and labels $\mathbf{Y} \in \mathbb{R}^{c \times n}$ like above. We are looking for the linear function $\mathbf{Y} = \mathbf{A}\mathbf{X}$. For this problem is equivariant under a group G , through two representations $u \in T_d(G)$ and $u_c \in T_c(G)$ acting on \mathbf{X} and \mathbf{Y} , respectively, it is sufficient for u and u_c to satisfy

$$u\mathbf{H}u^T = \mathbf{H} \quad u_c\mathbf{Y}\mathbf{X}^T u^T = \mathbf{Y}\mathbf{X}^T. \quad (15)$$

where $\mathbf{H} \equiv \frac{1}{n}\mathbf{X}\mathbf{X}^T$ is the covariance matrix of the input.

Theorem 1

Proof: [Theorem 1] The equivariance condition equation 1 becomes

$$u_c\mathbf{Y} = u_c\mathbf{A}\mathbf{X} = \mathbf{A}u\mathbf{X} \quad \Rightarrow \mathbf{A} = u_c\mathbf{A}u^{-1} \quad (16)$$

Assuming that the number of samples is much greater than features, $n \gg d$, and unbiased data, $\mathbf{X}^T\mathbf{X}$ will be full rank $d \times d$ and that its inverse exists. The solution to the linear regression $\mathbf{Y} = \mathbf{A}\mathbf{X}$ is given by $\mathbf{A} = \mathbf{Y}\mathbf{X}^T(\mathbf{X}\mathbf{X}^T)^{-1}$. Using the definition of covariance \mathbf{H} above, the condition equation 16 becomes $\mathbf{A} = u_c\mathbf{Y}\mathbf{X}^T u^T (u\mathbf{X}\mathbf{X}^T u^T)^{-1}$. Thus, a sufficient condition for equation 16 to hold is equation 15. \square

The first condition in equation 15 is unsupervised, stating that u preserves the covariance \mathbf{H} , while the second condition is supervised, stating that u_c and u preserve the cross-correlation of input and labels $\mathbf{Y}\mathbf{X}^T$. The group satisfying equation 15 is a subgroup of an orthogonal group, as we show below.

Corollary 1. *The subgroup of symmetries of linear regression satisfying $u\mathbf{H}u^T = \mathbf{H}$ in equation 15 form an orthogonal group isomorphic to $SO(d)$, with a Lie algebra basis given by*

$$L_i = \mathbf{H}^{1/2}L'_i\mathbf{H}^{-1/2} \qquad L'_i \in so(d) \qquad (17)$$

Corollary 1

Proof: multiplying $u\mathbf{H}u^T = \mathbf{H}$ by $\mathbf{H}^{-1/2}$ from both sides we see that $u' \equiv \mathbf{H}^{-1/2}u\mathbf{H}^{1/2}$ satisfies $u'u'^T = I$ meaning $u' \in SO(d)$. Expanding elements near identity we get $u \approx I + \epsilon \cdot L = \mathbf{H}^{1/2}(I + \epsilon' \cdot L')\mathbf{H}^{-1/2}$. Setting $\epsilon = \epsilon'$ proves equation 17. \square